Relating cone penetration resistance to sand state using the material point method

Martinelli, M.; Pisanò, F.

DOI
10.1680/jgele.21.00145

Publication date
2022

Document Version
Final published version

Published in
Geotechnique Letters (Online)

Martinelli, M. and Pisanò, F. (2022) ***Géotechnique Letters* 12**, 131–138, https://doi.org/10.1680/jgele.21.00145

Relating cone penetration resistance to sand state using the material point method

M. MARTINELLI*† and F. PISANÒ*

Cone penetration tests (CPTs) can quantitatively inform about the mechanical state of a sand. However, relating measured cone resistance values to sand state requires complex back-analysis of the processes occurring in the soil during the test. This paper provides new evidence of the value added in this area by modern large-deformation modelling based on the material point method (MPM). It is shown that accurate simulation of the relationship between cone resistance and sand state can be achieved, on condition that the constitutive behaviour of the soil – and especially its critical state features – is adequately modelled over a wide range of confining pressures. This study relies on the predictive capabilities of the critical state NorSand model, and shows how previous calibrations endeavours from the literature (based on triaxial test results) can support the MPM simulation of unrelated CPT results obtained through calibration chamber tests. MPM CPT simulations of ever-increasing quality will positively impact the state of the art of CPT interpretation procedures, to date still largely based on simplified cavity expansion theories.

KEYWORDS: in situ testing; numerical modelling; sands

NOTATION

C_u	uniformity coefficient
D_{50}	median particle diameter
e	void ratio
e_{cs}	void ratio at critical state
e_{max}	maximum void ratio
e_{min}	minimum void ratio
e_Γ	critical state line (CSL) parameter – exponential formulation
G	elastic shear modulus
G_s	specific gravity of particles
H	hardening parameter
H_i	($i = 1, 2, 3$) soil monitoring points in the material point method (MPM) model
I_r	rigidity index
K_0	at-rest earth pressure coefficient
N^*	hardening parameter
p	mean total stress
p'	mean effective stress
p_0	initial mean total stress
p'_0	initial mean effective stress
p_{ref}	reference pressure
Q	normalised cone resistance
q_c	cone resistance
r_c	cone radius in the MPM model
χ_{tc}	hardening parameter
Γ	CSL parameter – log-linear formulation
λ_c	CSL parameter – exponential formulation
λ_e	CSL parameter – log-linear formulation
ν	Poisson's ratio
ξ	CSL parameter – exponential formulation
σ'_{v0}	initial vertical effective stress
σ_{v0}	initial vertical total stress (= CC pressure)
ψ	state parameter
ψ_0	initial state parameter

Manuscript received 15 November 2021; accepted 2 February 2022.
Published online at www.geotechniqueletters.com on 4 April 2022.
*Faculty of Civil Engineering and Geosciences, Delft University of Technology, CN Delft, the Netherlands.
†Geo-Engineering Unit, Deltares, Delft, the Netherlands.

INTRODUCTION

Decades of geotechnical research have clearly pointed out the close relationship between the mechanical behaviour of sandy soils and their state. While such a state is fundamentally affected by numerous micromechanical and load-history factors, it is possible to gain broad insight into the behaviour of sand by acknowledging the combined influence of the current porosity and level of confinement (Bolton, 1986). A measure of soil state that has gained wide popularity in the interpretation/modelling of sand behaviour is the so-called 'state parameter' (ψ) introduced by Been & Jefferies (1985), which is defined as the difference between the current void ratio (e) and the critical state void ratio (e_{cs}) for the current value of the mean effective stress (p'). Quantitative relationships between ψ and specific features of behaviour could be established through extensive laboratory testing, although inevitably with an impact of the sample preparation procedure (Yimsiri & Soga, 2010). For this reason, in situ testing, particularly through the cone penetration test (CPT), is often preferred for characterising a soil in its natural site conditions. Cone resistance data, however, may not be easily converted into a reference state variable (e.g. ψ), which is in fact not directly measured during the test. As a consequence, a process of *a posteriori* interpretation is needed to quantitatively relate cone penetration resistance to soil state. In this respect, it is worth quoting Ghafghazi & Shuttle (2008), who noted that:

(*a*) the large deformations associated with the CPT, along with the non-linear behaviour of the soil and complicated boundary conditions, make this analysis an extremely difficult task
(*b*) nobody, to date, has provided a full numerical simulation of drained penetration that matches calibration data.

These considerations underlie the considerable amount of research that has been devoted to the study of (spherical)

cavity expansion as a simpler idealisation of the cone penetration process – a recent review is available in Huang *et al.* (2021). Cavity expansion solutions have been of increasing support to CPT interpretation, with an accuracy that is conditional on the inclusion of critical state principles in the constitutive modelling of sand (Shuttle & Jefferies, 1998; Cudmani & Osinov, 2001; Ghafghazi & Shuttle, 2008).

This study builds on the observation that, after over 10 years, the above statements by Ghafghazi & Shuttle (2008) are no longer fully accurate. In the last decade, remarkable achievements have been published about the large-deformation modelling of geotechnical penetration processes – for example, during a CPT. While Martinelli & Galavi (2021) have recently overviewed existing CPT simulation techniques, the proceedings of the last International Symposium on Cone Penetration Testing (CPT'18) testify their growing impact on site characterisation procedures (Hicks *et al.*, 2018).

The remainder of this study strengthens the belief that quantitative CPT interpretation strategies can be refined through direct large-deformation modelling of cone penetration – that is, without an intermediate cavity expansion analysis for the soil at hand. For this purpose, the potential of CPT modelling based on the material point method (MPM) is discussed, with emphasis on the role played by state-dependent sand modelling and the calibration of relevant material parameters. The accuracy of the adopted modelling framework is critically assessed against the results of calibration chamber (CC) tests in dry Toyoura sand from the literature (Fioravante *et al.*, 1991). It is worth stressing that the novelty of this study does not mainly relate to performing MPM-based CPT simulations, but, more importantly, to consistently using standard soil data to accurately predict CPT results and support their geotechnical interpretation. In fact, other numerical methods for large-deformation geoproblems, such as the particle finite-element method (PFEM) and the smoothed particle hydrodynamics (SPH), are also available, and could be applied to the analysis of CPTs in lieu of the MPM framework considered herein – see – for example, Monforte *et al.* (2018) and Bojanowski (2014).

NUMERICAL MODELLING OF CONE PENETRATION

This section covers the set-up of the MPM CPT model and the constitutive modelling of Toyoura sand's behaviour.

MPM model

Several recent studies support the suitability of MPM for the large-deformation analysis of penetration problems in soils, including pile installation (Kafaji, 2013; Phuong *et al.*, 2016; Galavi *et al.*, 2017, 2019) and CPT testing (Ceccato *et al.*, 2016; Ghasemi *et al.*, 2018). In this study, CPTs in a CC were numerically simulated using an MPM model in most respects similar to that described by Martinelli & Galavi (2021). The computational costs of all simulations were substantially reduced by exploiting the symmetry of the problem using a two-dimensional axisymmetric MPM code (Galavi *et al.*, 2018). The salient features of the code are (Martinelli & Galavi, 2021):

- dynamic MPM formulation, with the soil acceleration used as primary unknown variable (Jassim *et al.*, 2013)
- explicit, conditionally stable time integration, with automatic, CFL-based adaptation of the time step size
- simulation of cone–soil detachment and sliding by means of the contact algorithm by Bardenhagen *et al.* (2000)
- background mesh formed by three-node triangular elements with one integration point. The concept of 'moving mesh' was used to ensure fine discretisation around the cone–soil interface and accurate performance of the contact algorithm (Kafaji, 2013)
- sand behaviour reproduced using the state-dependent NorSand constitutive model (Jefferies, 1993). Its implementation in the MPM code features explicit Runge–Kutta time integration with automatic substepping and error control (Sloan *et al.*, 2001).

Additional computational aspects regarding mass scaling, numerical damping and mitigation of stress oscillations and volumetric locking are covered in Martinelli & Galavi (2021).

Figure 1 illustrates the numerical CPT model, featuring a perfectly rigid cone set to penetrate into an

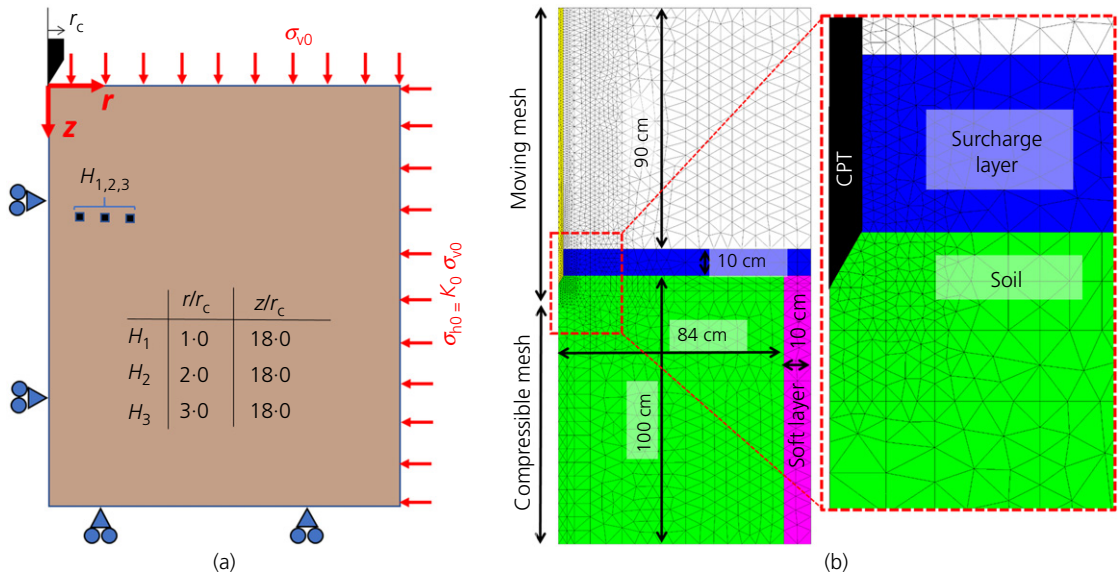

Fig. 1. Numerical CPT model: (a) geometry, boundary conditions, location of soil monitoring points ($H_{1,2,3}$); (b) background mesh for MPM calculations

Table 1. Index properties of Toyoura 160 sand

Grain description	Specific gravity of particle	Min/max void ratio	Median particle diameter	Uniformity coefficient
– Sub-angular	G_s: dimensionless 2·65	$e_{min} - e_{max}$: dimensionless 0·605–0·977	D_{50} (μm) 160	C_u: dimensionless 1·5

Source: from Ghafghazi & Shuttle (2008)

Table 2. Constitutive parameters of Toyoura 160 sand

Parameter			Value
Elasticity	I_r		equation (1)
	ν		0·2
Critical state	M_{tc}		1·28
	Log-lin CSL	Γ	0·983
		λ_e	0·019
	Exp CSL	e_Γ	0·934
		λ_c	0·019
		ξ	0·7
Hardening	N^*		0·41
	H		100
	χ_{tc}		4·4

Source: from Ghafghazi & Shuttle (2008) and Li & Dafalias (2000)

elasto-plastic soil. Cone radius ($r_c = 17{\cdot}85$ mm) and relevant boundary conditions are indicated in Fig. 1(a) along with the location of three soil monitoring points ($H_{1,2,3}$). The size of the soil domain and its background mesh (Fig. 1(b)) were set up after preliminary numerical tests (not reported for brevity), which overall confirmed that MPM results were accurate and free of undesired boundary effects. In all CPT simulation cases, the stress state was initialised with a soil pressure ratio K_0 equal to 0·5 (assumed reference value, Fig. 1(a)) under normally consolidated conditions (nil yield function). Two layers of elastic material were introduced to impose static boundary conditions – see Fig. 1(b): (*a*) the unit weight of the (blue) surcharge layer was in each case adjusted to enforce a given CC pressure, whereas a perfectly smooth contact between the layer and the rigid cone was introduced; (*b*) the (magenta) lateral layer was fixed on its outer edge and made very soft with a Young's modulus of 1 kPa – it was thus possible to maintain practically constant confinement around the inner soil mass (in green) during cone penetration.

NorSand modelling and parameter calibration

Resorting to a more sophisticated, ψ-dependent sand model was a necessary enhancement with respect to the study by Martinelli & Galavi (2021), which instead relied on the state-independent hardening soil model by Schanz *et al.* (1999). In particular, the version of NorSand described in Jefferies & Been (2016) was adopted in this study, with the sole difference of the Drucker–Prager form assumed for the plastic potential function (Jefferies & Shuttle, 2002). Building on the use of the state parameter ψ, NorSand complies with well-established critical state principles, and can spontaneously reproduce the transitions from contractive to dilative behaviour (and vice versa) that are known to occur in the vicinity of a penetrating cone (Ghafghazi & Shuttle, 2008).

To simulate the CC experiments performed by Fioravante *et al.* (1991), NorSand was calibrated for the Toyoura (160) sand used in the reference CPT tests – see the corresponding index properties in Table 1, as well as the compilation of CC test results provided by Jefferies & Been (2016). Such a calibration was facilitated by the study by Ghafghazi & Shuttle (2008), who identified the relevant NorSand parameters based on a dataset of triaxial compression test results – see Table 2. While the meaning of each NorSand parameter is explained in detail, for example, by Jefferies & Been (2016), some choices regarding the description of the elastic stiffness and the critical state line (CSL) require the following clarifications:

- at variance with Ghafghazi & Shuttle (2008)'s assumption, the rigidity index I_r (ratio between the elastic shear modulus G and p') was not set as a function of the (invariable) initial mean effective stress p'_0, but rather of the current value p' (Chaudhary *et al.*, 2004):

$$I_r = \frac{G}{p'} = 0{\cdot}878 \times \left(\frac{2{\cdot}17 - e}{1 + e}\right)^2 \left(\frac{p'}{p_{ref}}\right)^{-0{\cdot}47} \quad (1)$$

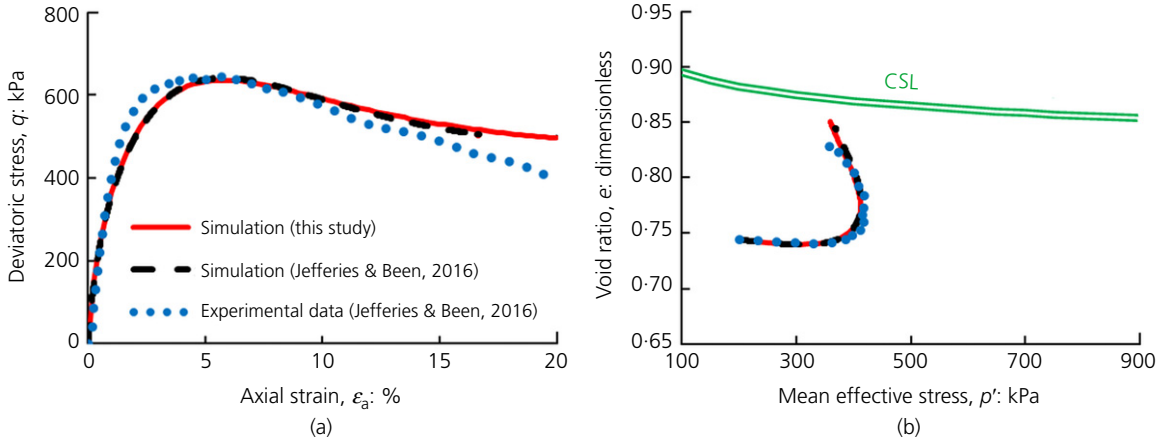

Fig. 2. NorSand model performance for a reference drained triaxial compression test (isotropic consolidation pressure: $p'_0 = 200$ kPa): (a) $q - \varepsilon_a$ response; (b) $e - p'$ response. Experimental data reported by Jefferies & Been (2016)

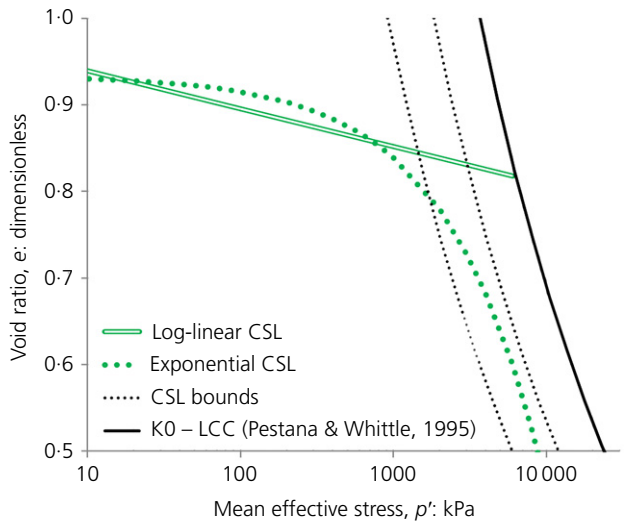

Fig. 3. Log-linear (equation (2)) against exponential (equation (3)) formulation of CSL of Toyoura sand

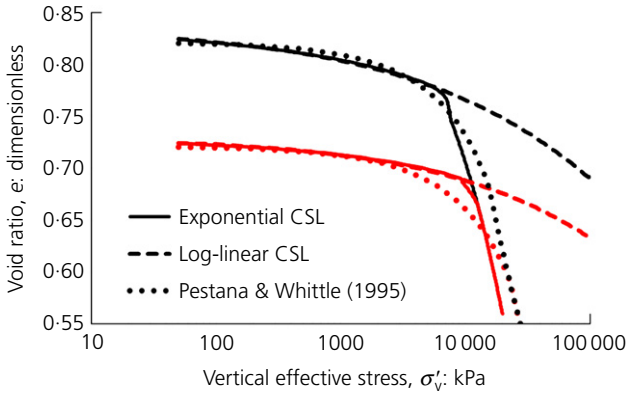

Fig. 4. NorSand simulation of oedometer compression tests on Toyoura sand with different CSL formulations (log-linear against exponential): comparison with the predictions of the compression model of Pestana & Whittle (1995)

with $p_{ref} = 100$ kPa. Such a choice was deemed more appropriate to reproduce the expected large variations in soil stiffness occurring during a CPT;

- the original NorSand features the following log-linear formulation of the CSL (Jefferies & Been, 2016):

$$e_{cs} = \Gamma - \lambda_e \ln\ (p') \tag{2}$$

where Γ and λ_e are CSL soil parameters (Table 2). In this study, the relationship between CSL formulation and simulated cone resistance was explored by comparing the MPM results obtained through two different CSL formulation, namely equation (2) and the following exponential formulation by Li & Wang (1998):

$$e_{cs} = e_\Gamma - \lambda_c \left(\frac{p'}{p_{ref}}\right)^{\xi} \tag{3}$$

- The values of the parameters e_Γ, λ_c and ξ are reported for Toyoura sand by Li & Dafalias (2000) (see Table 2).

With reference to the simulation of a triaxial compression test on Toyoura sand, Fig. 2 testifies the accuracy of the NorSand constitutive subroutine developed in this study: (*a*) it produces results similar to those returned by the implementation by Jefferies & Been (2016) (publicly distributed along with the reference publication) and (*b*) it captures Toyoura sand's triaxial behaviour in combination with the material parameters in Table 2 (log-linear CSL).

The description of the CSL locus has been widely recognised to play an important role in the modelling of sand compression, especially when a broad range of confining pressure is considered (Pestana & Whittle, 1995; Altuhafi *et al.*, 2018). Indeed, a CPT does induce large variations in p' in the surrounding soil, and possibly the occurrence of grain crushing (Arshad *et al.*, 2014). Even without attempting advanced modelling of sand crushing, it should be noted that standard triaxial compression tests – which guided the calibration of the parameters in Table 2 – do not induce stress paths, nor variations in p', similar to those experienced by the soil under/around a penetrating cone. Hence, the relevance of exploring the impact of alternative CSL formulations in MPM CPT simulations.

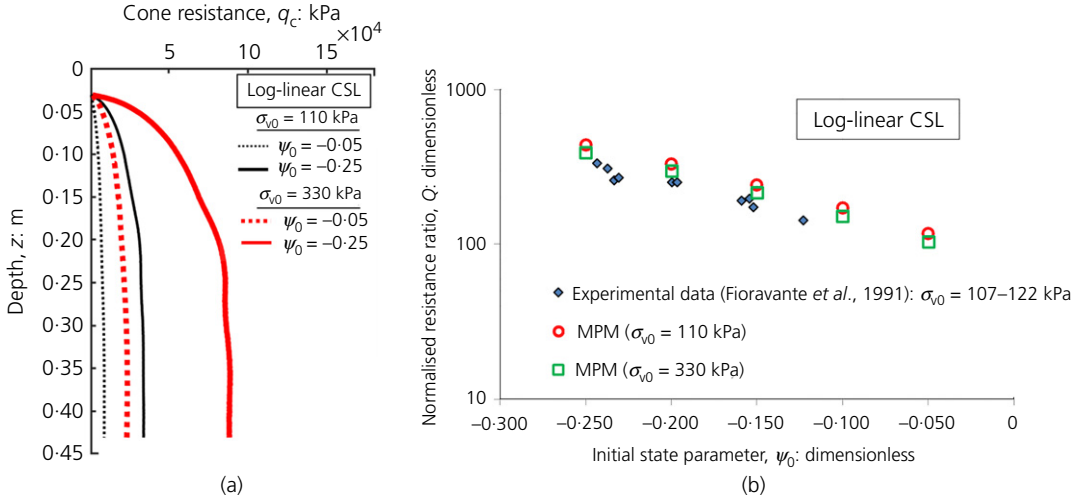

Fig. 5. MPM simulation of CPTs in Toyoura sand using a log-linear CSL (equation (2)): (a) q_c against penetration for $\psi_0 = -0{\cdot}25, -0{\cdot}05$ and $\sigma_{v0} = 110$ 330 kPa; (b) normalised cone resistance Q against initial state parameter ψ_0. CC data from Fioravante *et al.* (1991) – compiled and shared in electronic format by Jefferies & Been (2016)

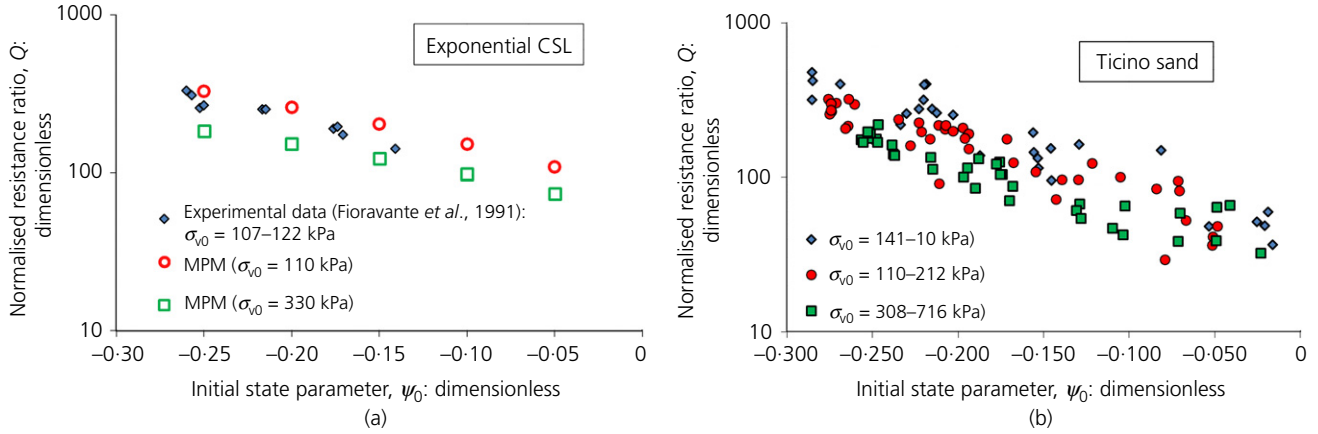

Fig. 6. Influence of the CC pressure on the $Q - \psi_0$ relationship: (a) MPM simulation of CPTs in Toyoura sand using an exponential CSL (equation (3)) – original CC data from Fioravante *et al*. (1991); (b) experimental $Q - \psi_0$ relationship for Ticino sand under a wide range of CC pressure – original CC data from Baldi *et al*. (1986). CC data compiled and shared in electronic format by Jefferies & Been (2016)

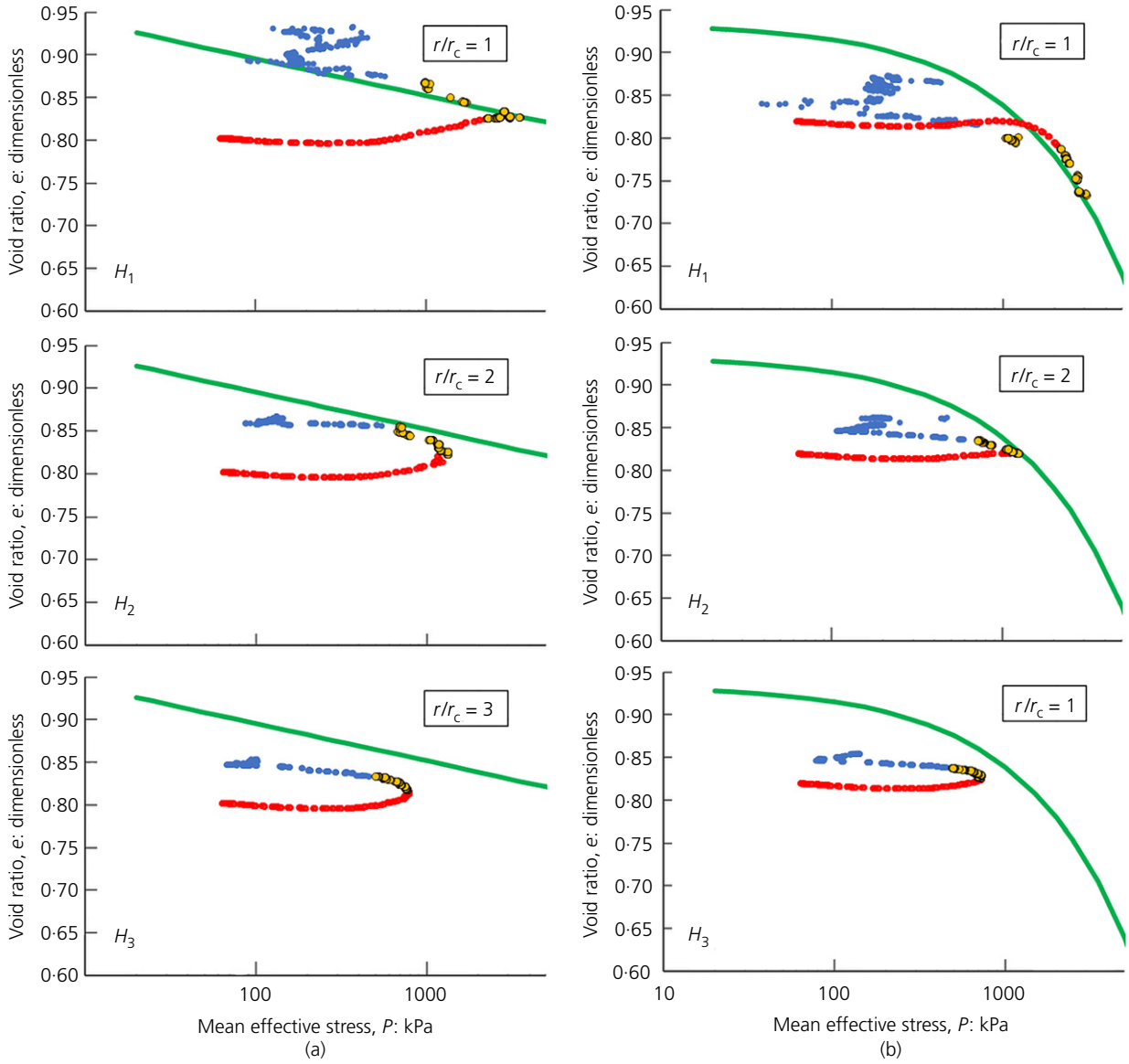

Fig. 7. MPM simulation of a CPT in Toyoura sand at low CC pressure – $\psi_0 = -0{\cdot}1$ and $\sigma_{v0} = 110\,\text{kPa}$. Simulated $e - p'$ paths at the monitoring points $H_{1,2,3}$ (Fig. 1(a)) associated with either a log-linear (a) or an exponential (b) CSL

The two CSLs obtained by introducing the Toyoura sand parameters (Table 2) into equations (2) and (3) are compared in Fig. 3. Calibration of the exponential CSL by Li & Dafalias (2000) appears to be fully consistent with the indicative 'CSL bounds' suggested by Robertson (2017) – that is, with a spacing ratio at high stresses between 2 and 4 with respect to the oedometer limit compression line (K_0-LCC – asymptotic line of the compression curve from oedometer compression at high stresses). The two CSLs return very similar values of critical void ratio for $10\,\text{kPa} < p' < 1000\,\text{kPa}$ (therefore with negligible impact on the triaxial simulation in Fig. 2), whereas significant differences emerge for $p' > 1000\,\text{kPa}$. An important consequence of the latter fact is exemplified in Fig. 4 in terms of the (different) oedometer responses that result at high stresses by adopting either equations (2) or (3) in the NorSand formulation. The exponential CSL produces oedometer simulation results in good agreement with the one-dimensional compression model proposed, and previously calibrated for Toyoura sand, by Pestana & Whittle (1995).

CPT SIMULATION RESULTS

The MPM simulation of CC tests in Toyoura sand was carried out after calibrating the NorSand model parameters as detailed above. It is remarked that such a calibration was completely based on existing interpretations of laboratory test results, without any later attempt to improve the agreement between CC data and MPM results.

Figure 5 reports the results of CPT MPM analyses performed in combination with the log-linear CSL in equation (2). The evolution of the tip resistance q_c with the penetration of the cone is shown in Fig. 5(a) for four CPT cases characterised by different values of the initial state parameter ($\psi_0 = -0{\cdot}25, -0{\cdot}05$) and the CC pressure ($\sigma_{v0} = 110$ and $330\,\text{kPa}$). In all cases, the cone resistance profile tends to a plateau after a penetration of approximately 30 cm, so that 40 cm was chosen as a reference depth for determining numerical q_c values. More MPM results are compared in Fig. 5(b) with the CC data of Fioravante *et al.* (1991), however, all associated with a narrow range of CC pressure ($\sigma_{v0} = 107$–122 kPa) and a cone radius of 35·7 mm. Both experimental and numerical results exhibit a nearly

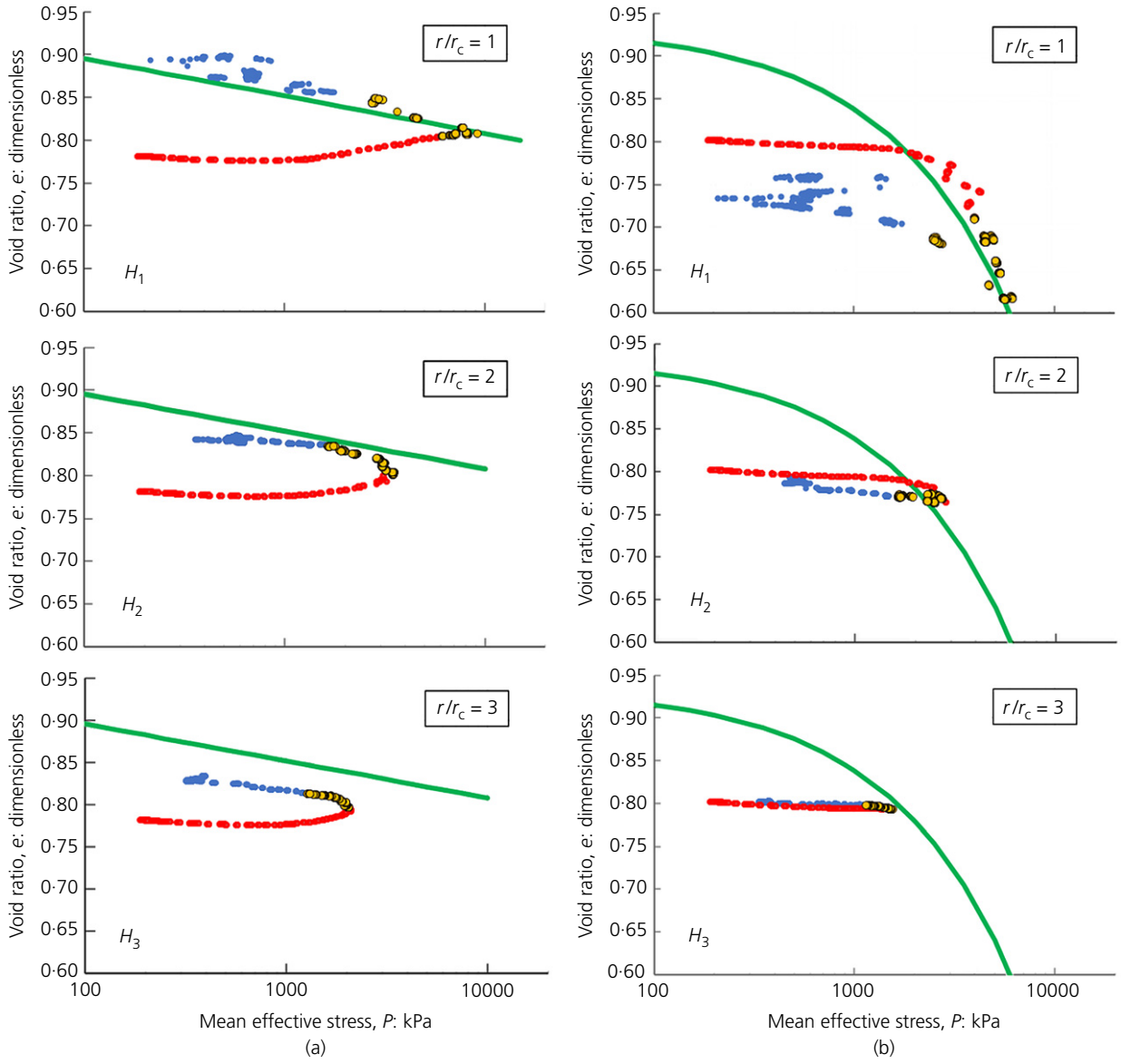

Fig. 8. MPM simulation of a CPT in Toyoura sand at high(er) CC pressure – $\psi_0 = -0{\cdot}1$ and $\sigma_{v0} = 330\,\text{kPa}$. Simulated $e - p'$ paths at the monitoring points $H_{1,2,3}$ (Fig. 1(a)) associated with either a log-linear (a) or an exponential (b) CSL

log-linear relationship between normalised cone resistance (Q) and initial state parameter (ψ_0) (Ghafghazi & Shuttle, 2008), with Q defined as proposed by Been *et al.* (1986, 1987):

$$Q = \frac{q_c - p_0}{p'_0}, \quad p_0^{(\prime)} = \frac{1 + 2K_0}{3}\sigma_{v0}^{(\prime)} \tag{4}$$

where $\sigma'_{v0} = \sigma_{v0}$ and $p'_0 = p_0$ for a dry sand.

Overall, the MPM results in Fig. 5(b) overpredict, though not dramatically, the measured Q values, with very limited impact of an increase in CC pressure from 110 to 330 kPa. In contrast, Fig. 6(a) clearly shows that the same increase in σ_{v0} affects substantially the normalised cone resistance if obtained using the exponential CSL in equation (3), in a way that seems more consistent with Q values measured under comparable CC pressures (in this case, $\sigma_{v0} = 110$ kPa – compare with Fioravante *et al.*, 1991). The notion of a lower normalised cone resistance at given ψ_0 and increasing CC pressure is also well supported by the experimental data of Baldi *et al.* (1986) in Fig. 6(b), which relate to CC measurements in Ticino sand for a broader range of CC pressure (σ_{v0} = 41–716 kPa). It is worth clarifying that the CC data points of Fioravante *et al.* in Figs 5(b) and 6(a) have been plotted against ψ_0 values obtained using that the same CSL formulations as in the associated MPM simulations – that is, equations (2) and (3), respectively.

Further insight into the influence of the CC pressure and the adopted CSL formulation is provided by Figs 7 and 8, where the $e - p'$ paths computed at the monitoring points in Fig. 1(a) ($H_{1,2,3}$) are shown for the same initial ψ_0 but different σ_{v0}. Such paths are drawn using a sequence of red, yellow and blue markers, which indicate the current position of the cone tip being above, beside and below the monitoring points, respectively. Both figures show that the soil around the penetrating cone experiences p' values in excess of 1 MPa at several locations, which confirms the limited applicability of a log-linear CSL (Maki *et al.*, 2014; Robertson, 2017). However, the effect of the CSL curvature may overall be modest in a relatively loose sand under low CC pressure, as is suggested by Fig. 7 – note, for example, the similar $e - p'$ paths obtained in the two cases at points H_2 and H_3. In contrast, a CSL that is inaccurate at high stresses has a strong impact on the simulated cone resistance as denser sand under higher CC pressure is considered. This statement is corroborated by Fig. 8, where completely different $e - p'$ paths are displayed depending on the adopted CSL expression – compare the dilative responses obtained for the log-linear CSL (Fig. 8a) and the contractive–dilative transitions associated with the exponential formulation (Fig. 8b).

CONCLUSIONS

This study has confirmed the maturity of MPM as a quantitative tool for the interpretation of CPTs in sand, for instance, to establish practical relationships between cone resistance and soil state without performing specific CC tests for the soil at hand. The comparison to CC test results in Toyoura sand from the literature has pointed out the key role played by the constitutive modelling of the soil, which needs to be state-dependent and accurate over a wide range of mean effective stress. In the latter respect, the choice of the CSL formulation has proven essential: its calibration should not be solely based on triaxial compression data at low confinement, but must be such to reproduce the compressibility of the soil up to very large stresses.

The conclusions drawn in this study will be further validated against a larger set of CC test results already available in the literature. This endeavour will require more detailed modelling of grain crushing, particularly of its impact on the stiffness, strength and dilatancy of sand.

DATA AVAILABILITY STATEMENT

Some or all data used are available from the corresponding author by request.

ACKNOWLEDGEMENTS

This research study is an outcome of a research project sponsored by the Dutch Ministry of Economic Affairs (Topsector Energiesubsidie) – grant number: TEWZ118001. The financial/technical support provided by Fugro NL Land B.V. and Siemens Gamesa Renewable Energy B.V. are gratefully acknowledged. The important contribution of Karel van Dalen and Maxim Segeren (TU Delft) is also warmly appreciated. All MPM simulations were carried out using a version of the Anura3D code (www.anura3D.com) developed at Deltares.

REFERENCES

Altuhafi, F. N., Jardine, R. J., Georgiannou, V. N. & Moinet, W. W. (2018). Effects of particle breakage and stress reversal on the behaviour of sand around displacement piles. *Géotechnique* **68**, No. 6, 546–555, https://doi.org/10.1680/jgeot.17.P.117.

Arshad, M., Tehrani, F., Prezzi, M. & Salgado, R. (2014). Experimental study of cone penetration in silica sand using digital image correlation. *Géotechnique* **64**, No. 7, 551–569, https://doi.org/10.1680/geot.13.P.179.

Baldi, G., Bellotti, R., Ghionna, V., Jamiolkowski, M. & Pasqualini, E. (1986). Interpretations of cpts and cptus, part II: drained penetration of sands. In *Proceedings of the 4th international geotechnical seminar on field instrumentation and in situ measurements* (ed. B. B. Broms), pp. 25–27. Singapore: Nanyang Technological Institute.

Bardenhagen, S., Brackbill, J. & Sulsky, D. (2000). The material-point method for granular materials. *Comput. Methods Appl. Mech. Engng* **187**, No. 3–4, 529–541.

Been, K. & Jefferies, M. G. (1985). A state parameter for sands. *Géotechnique* **35**, No. 2, 99–112, https://doi.org/10.1680/geot.1985.35.2.99.

Been, K., Crooks, J., Becker, D. & Jefferies, M. (1986). The cone penetration test in sands: part I, state parameter interpretation. *Géotechnique* **36**, No. 2, 239–249, https://doi.org/10.1680/geot.1986.36.2.239.

Been, K., Jefferies, M., Crooks, J. & Rothenburg, L. (1987). The cone penetration test in sands: part II, general inference of state. *Géotechnique* **37**, No. 3, 285–299, https://doi.org/10.1680/geot.1987.37.3.285.

Bojanowski, C. (2014). Numerical modeling of large deformations in soil structure interaction problems using fe, efg, sph, and mm-ale formulations. *Arch. Appl. Mech.* **84**, No. 5, 743–755.

Bolton, M. (1986). The strength and dilatancy of sands. *Géotechnique* **36**, No. 1, 65–78, https://doi.org/10.1680/geot.1986.36.1.65.

Ceccato, F., Beuth, L., Vermeer, P. A. & Simonini, P. (2016). Two-phase material point method applied to the study of cone penetration. *Comput. Geotech.* **80**, 440–452.

Chaudhary, S. K., Kuwano, J. & Hayano, Y. (2004). Measurement of quasi-elastic stiffness parameters of dense Toyoura sand in hollow cylinder apparatus and triaxial apparatus with bender elements. *Geotech. Test. J.* **27**, No. 1, 23–35.

Cudmani, R. & Osinov, V. (2001). The cavity expansion problem for the interpretation of cone penetration and pressuremeter tests. *Can. Geotech. J.* **38**, No. 3, 622–638.

Fioravante, V., Jamiolkowski, M., Tanizawa, F. & Tatsuoka, F. (1991). Results of CPTs in Toyoura quartz sand. In *Proceedings of the 1st international symposium on calibration chamber testing (ISOCCT-1)* (ed. A. B. Huang), pp. 135–146. New York, NY, USA: Elsevier.

Galavi, V., Beuth, L., Coelho, B. Z., Tehrani, F. S., Hölscher, P. & Van Tol, F. (2017). Numerical simulation of pile installation in saturated sand using material point method. *Procedia Engng* **175**, 72–79.

Galavi, V., Tehrani, F., Martinelli, M., Elkadi, A. & Luger, D. (2018). Axisymmetric formulation of the material point method for geotechnical engineering applications. In *Numerical methods in geotechnical engineering IX: proceedings of the 9th European conference on numerical methods in geotechnical engineering (NUMGE 2018), 25–27 June, 2018, Porto, Portugal* (eds A. S. Cardoso, J. L. Borges, P. A. Costa, A. T. Gomes, J. C. Marques and C. S. Vieira). Leiden, The Netherlands: CRC Press.

Galavi, V., Martinelli, M., Elkadi, A., Ghasemi, P. & Thijssen, R. (2019). Numerical simulation of impact driven offshore monopiles using the material point method. In *The XVII European conference on soil mechanics and geotechnical engineering* (eds H. Sigursteinsson, S. Erlingsson and B. Bessason), pp. 1–6. Reykjavik, Iceland: The Icelandic Geotechnical Society.

Ghafghazi, M. & Shuttle, D. (2008). Interpretation of sand state from cone penetration resistance. *Géotechnique* **58**, No. 8, 623–634, https://doi.org/10.1680/geot.2008.58.8.623.

Ghasemi, P., Calvello, M., Martinelli, M., Galavi, V. & Cuomo, S. (2018). MPM Simulation of CPT and model calibration by inverse analysis. In *Cone penetration testing 2018: proceedings of the 4th international symposium on cone penetration testing (CPT'18)* (eds M. A. Hicks, F. Pisanò and J. Peuchen), p. 295. Leiden, The Netherlands: CRC Press.

Hicks, M. A., Pisanò, F. & Peuchen, J. (2018). Cone penetration testing 2018. *Proceedings of the 4th international symposium on cone penetration testing (CPT'18)* (eds M. A. Hicks, F. Pisanò and J. Peuchen), p. 295. Leiden, The Netherlands: CRC Press.

Huang, M., Tong, S. & Shi, Z. (2021). Solution for spherical cavity expansion in state-dependent soils. *Acta Geotech.* **16**, No. 6, 1773–1788.

Jassim, I., Stolle, D. & Vermeer, P. (2013). Two-phase dynamic analysis by material point method. *Int. J. Numer. Anal. Methods Geomech.* **37**, No. 15, 2502–2522.

Jefferies, M. (1993). Norsand: a simple critical state model for sand. *Géotechnique* **43**, No. 1, 91–103, https://doi.org/10.1680/geot.1993.43.1.91.

Jefferies, M. & Been, K. (2016). *Soil liquefaction: a critical state approach*, 2nd edn. Boca Raton, FL, USA, CRC Press.

Jefferies, M. & Shuttle, D. (2002). Dilatancy in general Cambridge-type models. *Géotechnique* **52**, No. 9, 625–638, https://doi.org/10.1680/geot.2002.52.9.625.

Kafaji, I. K. (2013). *Formulation of a dynamic material point method (MPM) for geomechanical problems*. Ph.D. thesis, University of Stuttgart.

Li, X. S. & Dafalias, Y. F. (2000). Dilatancy for cohesionless soils. *Géotechnique* **50**, No. 4, 449–460, https://doi.org/10.1680/geot.2000.50.4.449.

Li, X. S. & Wang, Y. (1998). Linear representation of steady-state line for sand. *J. Geotech. Geoenviron. Engng* **124**, No. 12, 1215–1217.

Maki, I. P., Boulanger, R. W., DeJong, J. T. & Jaeger, R. A. (2014). State-based overburden normalization of cone penetration resistance in clean sand. *J. Geotech. Geoenviron. Engng* **140**, No. 2, 04013006.

Martinelli, M. & Galavi, V. (2021). Investigation of the material point method in the simulation of cone penetration tests in dry sand. *Comput. Geotech.* **130**, 103923.

Monforte, L., Arroyo, M., Carbonell, J. M. & Gens, A. (2018). Coupled effective stress analysis of insertion problems in geotechnics with the particle finite element method. *Comput. Geotech.* **101**, 114–129.

Pestana, J. M. & Whittle, A. (1995). Compression model for cohesionless soils. *Géotechnique* **45**, No. 4, 611–631, https://doi.org/10.1680/geot.1995.45.4.611.

Phuong, N., Van Tol, A., Elkadi, A. & Rohe, A. (2016). Numerical investigation of pile installation effects in sand using material point method. *Comput. Geotech.* **73**, 58–71.

Robertson, P. (2017). Evaluation of flow liquefaction: influence of high stresses. In *Proceedings of the 3rd international conference on performance based design (PBD-III)*. Vancouver, Canada: International Society for Soil Mechanics and Geotechnical Engineering.

Schanz, T., Vermeer, P. & Bonnier, P. (1999). The hardening soil model: formulation and verification. *Beyond 2000 in computational geotechnics* (ed. R. B. J. Brinkgreve), pp. 281–296. Rotterdam, The Netherlands: Balkema.

Shuttle, D. & Jefferies, M. (1998). Dimensionless and unbiased CPT interpretation in sand. *Int. J. Numer. Anal. Methods Geomech.* **22**, No. 5, 351–391.

Sloan, S. W., Abbo, A. J. & Sheng, D. (2001). Refined explicit integration of elastoplastic models with automatic error control. *Engng Comput. (Swansea)* **18**, No. 1/2, pp. 121–194, https://doi.org/10.1108/02644400110365842.

Yimsiri, S. & Soga, K. (2010). DEM Analysis of soil fabric effects on behaviour of sand. *Géotechnique* **60**, No. 6, 483–495, https://doi.org/10.1680/geot.2010.60.6.483.